Deep crustal geoelectric structure beneath the Northumberland Basin

Beamish, D., 1986. Deep crustal geoelectric structure beneath the Northumberland Basin, Geophysical Journal of the Royal Astronomical Society, 84, 619-640.

In back-catalogue of Geophysical Journal International.

doi: 10.1111/j.1365-246X.1986.tb04374.x

Summary.

In terms of lateral variations in conductivity structure, the southern Southern Uplands and Northumberland Basin are characterized by a region of attenuated vertical magnetic fields with small spatial gradients reflecting the presence of a substantial conducting zone. Five magnetotelluric data sets from the region have been analysed to provide accurate and unbiased estimates of the impedance tensor. The response data are used to investigate the deep geoelectric crustal structure of the region. Three appropriate sets of response data have been subjected to two construction algorithms for 1-D inversion. The geoelectric profiles recovered identify a deep crustal conducting zone underlying the Northumberland Basin. The zone, modelled as a layered structure, dips steeply from mid-crustal depths underneath the Northumberland Basin to lower crustal depths to the NW. The structure thus correlates, in location and geometry, with a deep crustal reflecting wedge detected offshore by a deep seismic reflection profile.

Introduction

Over the past five years a number of magnetotelluric experiments that include data sets from southern Scotland have been reported. The most complete are those by Jones & Hutton (1979a, b) and Ingham & Hutton (1982a, b). These papers also provide reference to magnetovariational studies that extend into parts of southern Scotland. The common features of these studies are a high-frequency limit of 10 s and a lack of observations across the Northumberland Basin and northern England. For present purposes these papers, together with the paper by Hutton, Ingham & Mbipom (1980), can be taken as providing a set of geoelectric crustal models that extend, in part, across southern Scotland. Jones & Hutton (1979b) provide one-dimensional (1-D) three-layer models for the crust and upper mantle at three widely-spaced sites in the Southern Uplands (BOR, NEW and PRE). The three-layer electrical geometry is one of resistor-conductor-resistor. The authors suggest, in conclusion, that the conductivity zone underlying the Southern Uplands is at a depth greater than 24 km , although there is evidence that the top interface of the zone might be closer to the surface to the SE (i.e. under NEW). The permitted resistivity of the conductive zone is in the range 29-90 ohm.m. Ingham & Hutton (1982a) provide three-layer, 1-D models at four sites (EAR, PEE, YAR and BOW) within the Southern Uplands and along a profile of measurements that extends NNW into the Grampian Highlands. The nine site profile was used to provide a 2-D geoelectric model (x = 400 km, z = 100 km). To the SE of the profile data, i.e. beneath the Northumberland Basin, the conductive zone extends vertically from 20 to 90 km and has a resistivity of order 75 ohm.m. The lack of observational control to the SE would suggest, however, that the model parameters in this region are not well constrained. Ingham & Hutton (1982b) provide an interpretation of the 2-D geoelectric profile by constructing crustal geotherms and identifying the likely mechanisms responsible for enhanced conductivity variations across the profile. Summarizing the tectonic implications of their interpretation, the authors indicate that the high conductivity under the Southern Uplands and the sharp boundary near the Southern Upland Fault does indicate that the region has special tectonic significance, although the existence of a subduction zone is not suggested by the model.

The essential problem, as with the results of magnetic variation experiments across the region (Banks, Beamish & Geake 1983; Banks & Beamish 1984), is one of depth resolution. There are many factors influencing the resolution of geoelectric structure obtained from an experimental data set. The prime constraint is provided by the instrumental bandwidth and this is necessarily coupled to the spatial density of measurement locations. If these are considered fixed, then the quality of our inferences concerning geoelectric structure will be governed by the accuracy of the electromagnetic response estimates obtained from the data set. The purpose of this study is to present further magnetotelluric results from five locations which span the Northumberland Basin, using an equivalent bandwidth to that of the former studies. The five site locations are shown in Fig. 1 in relation to geology and major crustal structures. The data processing adopted can be regarded as conventional with particular attention being paid to providing accurate and unbiased impedance estimates from large data sets.

The observed electromagnetic characteristics at the three central sites suggest that the gross geoelectric structure is approximately 1-D. The results from these sites are therefore used as a basis

for 1-D inversion to infer the vertical geoelectric crustal profile in the vicinity of the Northumberland Basin. A suitable strategy for the 1-D inversion of response data within the region is considered. The strategy adopted consists of restricting the bandwidth of the response data to the highest available frequencies and in forming the effective impedance. To alleviate the problems of non-uniqueness, two inverse construction algorithms are applied to the data. One of the algorithms permits the derivation of standard parameter statistics in the models obtained. Three-layer models with the configuration resistor-conductor-resistor are found to be optimum for the response data considered. The analysis identifies a highly conducting layer of resistivity 10 ohm.m of limited vertical extent, underlying the southern Southern Uplands and Northumberland Basin at mid- to lower-crustal depths. The accuracy of the response data at the three sites appears sufficient to define a spatially dependent depth to the conducting layer.

Because of the importance which the area has acquired in reconstructing the events associated with the closure of the lapetus Ocean during the lower Palaeozoic, a NW-SE profile defining the NW dip of the conducting zone is briefly considered in relation to current geological and geophysical models. The non-uniqueness found in such models suggests that the question of the physical properties responsible for the conducting zone may be considered an ill-posed problem, at present. When consideration is given to the structural significance of the conducting zone , however , it is possible to correlate the depth and geometry of the zone with a deep crustal reflecting wedge detected offshore by a deep seismic reflection experiment an d considered by Brewer et al . (1983) to be a likely signature of the lapetus suture zone.

Data and processing

The five-component magnetotelluric system is based on the EDA FM 1OOB fluxgate magneto- meter which provides Hx. Hy and Hz. The two telluric channels (Ex, Ey) are provided by a cross-arrangement of non-polarizing CuS04 electrodes separated by 100 m in the measurement directions. All five analogue data channels are subject to pre-conditioning consisting of (a) application of a low-pass anti-alias filter with a 3 dB attenuation level at 15 s; (b) application of a high-pass filter with a 3 dB attenuation level at 104 s; prior to 12-bit digitization and logging on digital cassette. The sampling interval was 10 s and continuous data runs were limited to 72 hr at each site. The instruments were deployed, as part of a wider geomagnetic experiment, at the five sites for a minimum recording time of one month. The resulting large data sets required some degree of reduction. For the purposes of analysis a minimum of 240 hr (10 days) of data was selected for each site on the basis of power spectral densities within individual records or data segments.

To provide results over the three decades 10-10^4 s it is advantageous to perform data averaging. A spectral scheme equivalent to that described by Beamish & Banks (1983) was employed.

The electric and magnetic field components are related, in the frequency domain, by the two equations:

$$Ex = Zxx \cdot Hx + Zxy \cdot Hy \quad (1)$$

$$Ey = Zyx \cdot Hx + Zyy \cdot Hy \quad (2)$$

The two pairs of impedance elements (Zxx,Zxy) and (Zyx,Zyy) are usually estimated by least-squares solutions which minimize noise on a particular data channel of the two input, one output linear relationships (Sims, Bostick & Smith 1971). For each equation, we can assume independent noise on three channels in turn and obtain three pairs of equations in the four unknowns. If we assume the three pairs of equations are independent, there are six independent combinations giving rise to six independent estimators for each element.

Despite attempts to provide a unified approach to combining such estimates (Sims et al 1971; Gundel 1977; Muller 1982), it is now increasingly common with no *a priori* information on the distribution of noise terms across the data channels, to provide two limiting cases of noise content (e.g. Adam & Vero 1976; Cox et al. 1980; Chave et al. 1981).

The first solution gives rise to downward-biased estimates of the impedance tensor **Z** as:

E = **Z H**

In which the source of bias derives only from noise terms in **H**. The second solution gives rise to upward-biased estimates of the impedance tensor **Q** derived from the admittance tensor **A** as:

H = A E , **Q**= $\mathbf{A}^{-1}$

In which the source of bias derives only from noise terms in **E**. The t rue values of each impedance element Tij are thus estimated from the upper and lower bounds provided by Zij and Qij , with random errors taken into account. Although derived from the same set of auto- and cross-spectra, the distributions of **Z** and **Q** should be treated independently since they are biased estimates of the true expectation values.

Bias reduction takes place by winnowing the full set of available estimators. The elements of **Z** and **Q** are estimated in pairs as per equations (1) and (2). The quality or signal/noise ratio of each pair of elements is estimated by the associated partial and/or multiple coherence function(s). The simplest form of winnowing takes place when pairs of estimators are rejected if their associated multiple coherence function (Υ^2) falls below a threshold. Typically if the data set provides an adequate distribution of high normalized multiple coherence functions (e.g. $\Upsilon^2 > 0.9$), bias errors can be reduced to the magnitude of random errors. The resulting population of individual estimates , together with their associated random errors, are used in a weighted least-squares regression to form weighted mean estimates and weighted estimates of the variance (and hence confidence limits) for all eight elements.

The efficiency of the procedure applied to a particular data set can be illustrated by plotting, in the complex plane, the final determinations (Zij and Qij) for a particular element, together with their associated standard errors. Both Zyx and Qyx determined for site 3 are plotted in this manner in Fig. 2. The 11 period bands shown cover the period range 7200 s (B1) to 30 s (B17). The larger magnitude result in each case is obtained from the estimate Qyx, the upward-biased result. If the phase of the result is a non-biased quantity, as is predicted, the two biased determinations should lie on a radial line passing through the origin. When random errors (the circles of confidence) are taken into account this behaviour is observed . It is apparent from Fig. 2 that, over the central part of the available bandwidth, bias errors are of the same order as or less than the 95 per cent confidence limits associated with the true expectation (Tyx) which lies in the interval:

$(|Z_{yx}| + \Delta Z_{yx}) <= |T_{yx}| <= (|Q_{yx}| + \Delta Q_{yx})$

where Δ denotes a standard error.

A number of different approaches to the estimation of the true expectation value are possible (Adam & Vero 1976; Cox et al. 1980; Jones, Olafsdottir & Tiikkainen 1983) when determinations of both Zij and Qij are available. The weighted average was adopted in the present study. As is indicated in Fig. 2, the estimates for the highest frequency band (B18) are strongly degraded by noise (at all sites) and are omitted from the following study.

Magnetotelluric results

Having obtained accurate and unbiased estimates of the impedance elements at each site, the impedance tensor was rotated to a principal direction and the standard magnetotelluric parameter set determined in the rotated coordinate system. The basic parameter set then consists of apparent resistivity and phase in the principal directions (maximum and minimum), the azimuth of the maximum rotation direction together with the associated parameters of skew, eccentricity and anisotropy ratio (Vozoff 1972). The results, omitting the latter two parameters, for the northernmost (site1 , EB) and southernmost (Site 5, PW) sites are displayed in Fig. 3(a, b). The equivalent results for the remaining three sites (sites 2, 3, and 4) are shown in Fig. 3(c, d , and e).

Considered in total, the five site magnetotelluric response curves exhibit similarities, particularly in the form of the phase curves. There is a tendency for the maximum apparent resistivity curve to approach the same value at long periods, at all five sites. The apparent discontinuities at site 5 (Fig. 3b) are due to the anisotropy ratio approaching zero. In detail, the impedance tensor available at each site is sufficiently well-determined to define significant differences across the region, particularly at the shortest periods. In terms of structural dimensionality, as indicated by the skewness coefficients, it is apparent that only the central three sites (sites 2, 3 and 4) have sufficiently low values (e.g. < 0.1) to warrant an initial premise of approximately 1-D structure. Even then, the skewness coefficients of these sites are significantly frequency dependent. Rather than develop further necessary, but not sufficient, conditions from each data set to provide an indication of structural dimensionality, it is instructive to examine the anomalous vertical field (the tipper) at various locations across the region. These are available across the same bandwidth but at many more locations within the study area. The amplitudes and azimuths of real and imaginary induction arrows at various locations across the area are shown in Fig. 4. In Fig. 4(a) the induction arrow results for site 1 are displayed. A strong frequency dependence is observed , indicating the near-field influence of the Southern Uplands Fault. In Fig. 4(b) the induction arrow results from nine sites in the central region of the Northumberland Basin have been overlaid. The nine sites include sites 2, 3 and 4 together with the site ESK (Fig. 1). A consistent set of low magnitudes, in both real and imaginary components, is observed. In Fig. 4(c), the induction arrow magnitudes for 10 sites confined to the Alston Block (Fig. 1) have been overlaid. The anomalous vertical field, at the 10 sites including site 5, appears strongly and consistently influenced by lateral variations in conductivity structure.

It is evident from this and other work (Banks & Beamish 1984) that, in contrast to the regions to the north and south the central Northumberland Basin is characterized by a zone of attenuated anomalous vertical fields possessing small spatial gradients . In view of the results presented, it is suggested that the 1-D inversion of the sounding curves at the central three sites appears justified.

Strategy for 1-D inversion

The region in question, the Eskdalemuir or Southern Uplands anomaly, has received close attention from the geomagnetic community with regard to the possible influence of current channelling on various data sets. The relevant work has been scrutinized by Jones (1983). He concludes that at periods less than about 1000 s, a 2-D model is certainly justifiable, and the existence of any channelled current is highly doubtful. The period at which doubt turns to certainty is adjustable, however, since the estimation of such a period (range) is a function of the geoelectric structure to be determined. Recent work on the problem of local and regional induction in the British Isles (Banks & Beamish 1984) would suggest a lower period bound for the applicability of strictly 2-D models. The authors suggest that in the period range 400-2000 s, the anomalous vertical fields, at least, are determined by currents induced in a thin-sheet of laterally varying conductance comprising the shelf-seas and their underlying sediments together with the onshore extensions of the sedimentary basins. In the light of such discussion, the present study adopts the simple expedient of restricting the period range (T) over which the data sets are inverted to $T < 400$ s. In practice such a procedure does not prove restrictive in that any deep layered resistivity structure has a negligible influence on the response at sufficiently high frequencies.

The tensor nature of the impedance elements allows one to obtain apparent resistivity curves at any selected horizontal azimuth. The apparent resistivity curves shown in Fig. 3 are presented in the maximum and minimum principal directions and, as the results demonstrate, the principal direction is generally a stable function of frequency and is significantly different at all five sites. The rotation to principal directions is often viewed as approximately providing the two limiting resistivity curves (TE and TM) that would be generated by a strictly 2-D earth. If one can identify the TE and TM modes from the data set, it is possible to make a suitable choice of azimuthal apparent resistivity curve on which to perform a 1-D inversion provided there is some pre-defined model of geoelectric structure, be it 2-D (e.g. Reddy & Rankin 1972) or 3-D (e.g. Berdichevsky & Dimitriev 1976). Clearly any such approach should also be consistent with the structural information provided by the anomalous vertical field. As demonstrated in Fig. 4, the azimuthal information provided by the induction arrows in the region of the Northumberland Basin (Fig. 4b) is both frequency dependent and spatially variable. In such circumstances it is difficult to adopt a consistent synthesis of the available azimuthal information in terms of the definition of TE and TM modes. To alleviate this problem, the apparent resistivity curve obtained from the rotationally invariant , effective impedance:

$$Z_E = (Zxy - Zyx)/2$$

has been used.

Having defined a consistent set of response data to be inverted it is necessary to consider the construction of an appropriate algorithm for the inverse problem. In general, the 1-D inversion of magnetotelluric data is usually treated within a framework that employs a linear approximation to the non-linear problem . The uniqueness of any solution obtained can then be questioned and the importance of using a variety of construction algorithms to assess uniqueness has recently been stressed (Oldenburg, Whittal & Parker 1984).

The three response data sets (sites 2, 3 and 4) have been subjected to two different inversion algorithms. The first scheme devised by Fischer et al. (1981) and Fischer & Le Quang (1981) has two parts. The first stage is a downward-moving algorithm that recovers the geoelectric profile in terms of successive layers by a direct (analytic) procedure. The second stage uses this model (or modified model) as input to an efficient minimization procedure that locates an absolute minimum of the misfit without recourse to parameter derivatives. The original papers by Fischer et al. (1981) and Fischer & Le Quang (1982) give a full account of the algorithms and their implementation, and only a brief description is given here. The measure of misfit between measured and calculated response curves as defined by the standard deviation EPS (Fischer et al . 1981, equation 5) together with the authors' adopted weighting schemes were used. The parameter space explored is necessarily a function of any parameter constraints applied and the number of layers utilized. In applying the algorithm, resistivities were restricted to the range 1-106 ohm.m, and the appropriate number of layers was investigated using the procedure suggested by Fischer & Le Quang (1981). It appears that over the bandwidth, 30-400 s, three-layer models form the simplest parameter set with an appropriate minimum in the standard deviation. The optimum (best-fit) three-layer models, obtained for each site, are considered later.

The second inversion algorithm considered was that of ridge regression or damped least- squares. The method is strongly dependent on parameter derivatives; recent general reviews are given by Hoversten , Dey & Morrison (1982) and Lines & Treitel (1984). A minimum norm solution is approached using successive iterations . The ridge regression method (Levenberg 1944; Marquardt 1970) stabilizes the iteration procedure. The statistical parameters we use to characterize the model are parameter standard errors and parameter correlation coefficients.

The parameter standard errors are defined as the square root of the diagonal terms of **V**, the parameter covariance matrix , and the correlation matrix is the diagonally normalized covariance matrix:

$$Cij = Vij / ((Vii)^{1/2} (Vjj)^{1/2})$$

The correlation coefficients, thus defined, measure the linear dependence between parameters. If an element Cij is close to ± 1 then the i'th and j'th parameters exhibit strong linear dependence. If Cij represents the correlation between thickness (t) and resistivity (ρ) of a layer then if Cij = + 1, only the ratio t/ρ is well-determined, conversely if Cij = -1 only the product tρ is well-determined. If the correlations are small then the standard errors are a good measure of the uncertainty in each parameter. If, however, two parameters are highly correlated then the standard errors will be larger than the actual uncertainties as discussed by Inman (1975).

An adequate start model is required to initiate the inversion procedure. The start models were obtained as three-layer models constructed using the Bostick inversion (Bostick 1977; Weidelt et al. 1980). In contrast to the previous inversion scheme, model resistivity values were unconstrained.

Results of 1-D inversion

The results of the two construction algorithms applied to the three data sets are given in Table l (a, b, c). Solution 1 refers to the parameters obtained using the procedures of Fischer et al . (1981) and Fischer & Le Quang (1981). Solution 2 refers to the parameters and statistics obtained using ridge

regression. A consistent measure of misfit of the final solutions is provided by the chi-square statistic (Parker 1983). The solutions obtained are marginally acceptable at the 95 per cent confidence limit (chi-square = 27). The parameter correlation matrices are also shown in Table 1. As expected, for a highly conducting layer (such as layer 2), they display a consistent positive correlation, close to unity, in the parameter pair ρ2 , t2 at all three sites. Clearly the vertical conductance of layer 2 is the best resolved feature of the model and the standard errors of ρ2 , t2 are conservative estimates of the true errors.

The results of the two inversion procedures on the data at the three sites are plotted in logarithmic/linear coordinates in Fig. 5(a, b, c). The dotted line refers to solution 1 while the dashed line refers to solution 2. The shaded region defines the standard error in the parameters obtained from solution 2 and as such is a linear confidence region that ignores multiparameter correlations. In the case of the parameters relating to the definition of the highly conducting layer (ρ2 , t2), the standard errors are conservative estimates; the actual errors being much less than those indicated.

Apart from parameter ρ1, the two inversion procedures produce consistent results in all other parameters. The optimum value of the resistivity of the highly conducting layer (HCL) is clearly 10 ohm.m while the depth of this layer must be viewed as a function of location. The resistivity of layer 3 is consistent at all three sites having a geometric mean , over the six estimates, of 229 ohm.m. There is an apparent wide range of resistivity values for layer 1 between the three sites. The resolution of this layer is, however, highly dependent on the high-frequency asymptotic behaviour of the observed response which, in the present case, is limited. It is very unlikely that the resistivity values indicated for ρ1 apply throughout the depth ranges shown. We restrict our attention instead to the parameters defining the HCL at all three sites, i.e. t1, ρ2 , t2 . Before discussing the results obtained it is worth examining the models obtained from several other inversion schemes applied to a magnetotelluric data set from Newcastleton (NEW, Fig. 1).

As part of the COPROD test (Comparative study of methods of deriving the conductivity Profile within the Earth from One dimensional magnetotelluric Data) organized by A. G. Jones, a response set from NEW (Jones & Hutton 1979a) was subjected to a number of inversion schemes. The response set consisted of 23 estimates of apparent resistivity and phase, with 15 well-estimated data pairs between 28.5 and 1960.8 s. Three main differences exist between the NEW response and those of the present study: (a) The NEW response was derived only from solution (I,2) and is therefore downward-biased; (b) the NEW response that was modelled extends to much longer periods ; (c) the NEW response that was modelled consisted of rotated results along the major axis of the rotation ellipse.

As stated previously, it is the vertically integrated conductance that is the best resolved feature of any HCL. This conductance, together with the depth to the HCL is therefore used for the comparison. The 'best-fitting', three-layered models presented by various authors have been chosen; layer 2 then defines an HCL above a uniform half-space. Four published results are compared with the equivalent results at all three locations of the present study in Table 2. Given the large differences in location , data and inversion schemes, the comparison is encouraging. Despite the lower values of conductance obtained for the NEW data, which may be real or the effect of bias, the results confirm the presence of a pervasive HCL of limited vertical extent within the crust underlying the southern Southern Uplands and Northumberland Basin .

Discussion

The data sets and analysis of the present study have identified a highly conducting crustal layer (HCL) beneath the southern Southern Uplands and Northumberland Basin. The consistency and resolution of the two inversion procedures suggests that the accuracy of the response data at the three sites is sufficient to define a spatially dependent depth to the HCL. The layered parameterization may not be physically real, however if a particular model is acceptable then the resistivity values must undergo some form of excursion over the depth range indicated. Since the optimum models define a resistivity of about 10 ohm.m for the HCL at all three sites, it is suggested that it is the same layer (or resistivity excursion) underlying the study region.

The depth of the HCL with site locations projected on a NW, SE profile is shown in Fig. 6 in relation to two other recent crustal models. In the SE, the velocity layers under northern England presented by Bott , Swinburn & Long (1984) are shown. To the NW and underlying the Southern Uplands proper is a recent model proposed by Leggett, McKerrow & Soper (1983) to explain the crustal evolution of southern Scotland in terms of the tectonics associated with Lower Palaeozoic subduction. In essence, the proposed model embodies the progress of the Southern Upland accretionary prism in response to the northward subduction of oceanic (Iapetus) material along the Solway Trench. The model then requires subsequent northward underthrusting and telescoping of continental basement to produce progressive southward imbrication of continental basement at lower crustal depths beneath the accretionary complex. Clearly the definition of the conductive zone at mid- to lower crustal levels should supply some constraints to this and other models of Lower Palaeozoic tectonics. In order to apply such constraints it is first necessary to establish a physical mechanism for the high conductivity zone.

Synthesizing the possible mechanisms for enhanced conductivity at such depths is a considerable exercise . It can be considered equivalent to identifying the physical properties responsible for deep seismic reflections. The two problems show a high degree of equivalence in that the physical properties requiring consideration occur on the microscopic scale and typically might involve the coupling of primary rock fabric parameters (e.g. pore space) with secondary rock parameters such as fluid inclusions, either bound or free. In addition, a mechanism for enhanced conductivity cannot be generated in isolation. As suggested in Fig. 6 current tectonic models for the region are complex and non-unique. Recent seismic models for the region (Hall et al . 1983) show considerable azimuthal variation, along and across the Caledonian strike, of P-wave velocities. The non-uniqueness of such models means that only marginal constraints may be applied in the interpretation of the causes of enhanced conductivity underlying the Southern Uplands, although it has been attempted (Ingham & Hutton l 982b). In terms of a mechanism for enhanced conductivity, one of the more forceful observational data sets is heat flow. The current Atlas of Geothermal Resources of the UK (Gale 1984) provides a broad heat flow value of 50 $mW.m^{-2}$ across most of the Southern Uplands and Northumberland Basin although actual heat-flow measurements in the locality are non-existent. If such a low crustal geotherm is realistic, it would indicate a zone of increased fluid concentration as a probable cause of the HCL if the arguments of Shankland & Ander (1983) are accepted.

Another forceful observational data set is provided by the BIRPS deep seismic reflection studies of the British Caledonides. When consideration is given to the structural significance of the HCL, an interesting comparison can be made with the F-E profile collected on the WINCH offshore traverse (Brewer et al. 1983). The NW- SE reflection profile (F-E) defines a parallel offshore traverse to the study region and reveals a non-reflecting upper crust above a very reflective lower crustal wedge with a strongly northward-dipping upper surface . The NW-SE onshore profile of enhanced conductivity shown in Fig. 6 appears to define an upper zone within the reflective wedge. The correlation between the two data sets is considered in detail by Beamish & Smythe (1986). Although the interpretation of a geoelectric profile by Ingham & Hutton (1982b) supported the hypothesis that the Highland Boundary Fault is the location of an ancient subduction zone, the present model argues for an association between the HCL and the deep reflective wedge and hence a likely basis for the definition of the Iapetus suture zone beneath the southern Southern Uplands and Northumberland Basin.

Acknowledgments

My grateful thanks go to Gaston Fischer for providing the coded algorithms for the 1-D inversion scheme used at Neuchatel, and also to John Riddick for the continued use of his soldering iron. This paper is published with the approval of the Director, British Geological Survey (NERC).

References

Adam , A. & Vero, J., 1976. Magnetotelluric data processing methods, in KAPG Geophys. Monogr. Geoelectric and Geothermal Studies , pp. 256-263, ed . Adam, A., Akademiai Kiado, Budapest.

Banks , R. J. & Beamish, D., 1 984 . Local and regional induction in the British Isles, Geophys. J. R. astr. Soc., 79, 539 -553.

Banks, R. J., Beamish, D. & Geake, M. J., 1983. Magnetic variation anomalies in northern England and southern Scotland, Nature. 303, 516 -518.

Beamish, D. & Banks, R. J., 1983. Geomagnetic variation anomalies in northern England: processing and presentation of data from a non-simultaneous array , Geophys. J. R. astr. Soc., 75, 513-539.

Beamish, D. & Smythe, D . K., 1986 . Geophysical images of the deep crust : the Iapetus Suture, J. geol. Soc. London , submitted.

Berdichevsky , M. N. & Dmitriev, V. I., 1976. Basic principles of interpretation of magnetotelluric sounding curves, in KAPG Geophys. Monogr., Geoelectric and Geothermal Studies , pp. 165-221, ed . Adam , A . Akademiai Kiado , Budapest.

Bostick, r. X., 1977. A simple almost exact method of MT analysis, Workshop on Electric Methods in Geothermal Exploration , U.S. Geol. Surv., Contract No. 14080001-8-359.

Bott, M. H. P., Swinburn, P. M . & Long, R. E., 1984. Deep structure and origin of the Northumberland and Stainmore troughs, Proc. Yorks. geol. Soc., 44, 4 79-495.

Brewer, J. A., Matthews, D. H., Warner, M. R., Hall, J ., Smythe , D. K. & Whittington, R. J., 1983. BIRPS deep seismic reflection studies of the British Caledonides, Nature , 305, 206-210.

Chave, A. D., von Herzen, R. P., Poehls, K. A. & Cox, C. S., 1981. Electromagnetic induction fields in the deep ocean north-east of Hawaii: implications for mantle conductivity and source fields, Geophys. J. R. astr. Soc., 66 , 379-406.

Cox, C. S., Filloux , J . H., Gough , D. L, Larsen , J. C., Poehls, K . A., von Herzen, R. P. & Winter, R ., 1980 . Atlantic lithospheric sounding, in Electromagnetic induction in the Earth and Moon , pp. 13-22, ed . Schmucker, U., Centr. Acad. Publ. Japan, Tokyo and Reidel, Dordrecht.

Fischer, G. & Le Qua ng, B. V., 1981. Topography and minimization of the standard deviation in one-dimensional magnetotelluric modelling, Geophys. J. R. astr. Soc ., 67, 279-297.

Fischer, G., Schnegg, P. A., Peguiron, M. & Le Quang, B. V., 1981 . An analytical one-dimensional magnetotelluric inversion scheme, Geophys. J. R. astr. Soc., 67, 257-278.

Gale, I. N., 1984. Atlas of the Geothermal Resources of the United Kingdom , Invest. Geotherm. Potent, UK, British Geological Survey.

Gundel, A., 1977. Estimation of transfer functions with reduced bias in geomagnetic induction studies, Acta Geodaet. Geophys. Montanist. , 12, 345-352.

Hall, J., Powell, D. W., Warner, M. R., El-Isa , Z. H., Adesanya , 0. & Bluck , B. J ., 1983. Seismological evidence for shallow crystalline basement in the Southern Uplands of Scotland , Nature, 305, 418-420.

Hoversten, G. M ., Dey , A. & Morrison, H. 17., 1982. Comparison of live least-squares inversion techniques in resistivity sounding, Geophys. Prospect ., 30, 688 -715.

Hutton , V. R. S., Ingham , M. R. & Mbipom , E. W., 1 980. An electrical model of the crust and upper mantle in Scotland, Nature, 287, 30 -33.

Ingham, M. R. & Hutton, V. R . S., I 982a. Crustal and upper mantle electrical conductivity structure in Southern Scotland, Geophys. J. R. astr. Soc., 69, 579 -594.

Ingham , M. R. & Hutton, V. R. S., 1982b. The interpretation and tectonic implications of the geoelectric structure of Southern Scotland, Geophys. J. R. astr. Soc., 69, 595-606.

Inman, 1. R., 1975. Resistivity inversion with ridge regression, Geophysics, 40, 798-817.

Jones, A. G., 1983. The problem of current channelling: a critical review, Geophys. Surveys, 6, 79-122.

Jones, A. G. & Hutton , R., l 979a. A multi-station magnetotelluric study in southern Scotland - I. Fieldwork, data analysis and results, Geophys. J. R. astr. Soc., 56 , 329-349.

Jones, A. G. & Hutton, R., 1979b. A multi-station magnetotelluric study in southern Scotland - II. Monte-Carlo inversion of the data and its geophysical and tectonic implications, Geophys J. R. astr. Soc., 56, 351-368.

Jones, A. G., Olafsdottir, B. & Tiikkainen, J., 1983. Geomagnetic induction studies in Scandinavia, J. Geophys., 54 , 35-50.

Larsen, J. C., 1981. A new technique for layered Earth magnetotelluric inversion, Geophysics, 46, 1247- 1257.

Leggett, J. K., McKerrow, W. S. & Soper, N. 1., 1983. A model for the crustal evolution of southern Scotland, Tectonics, 2, 187-210.

Levenberg, K., 1944. A method for the solution of certain nonlinear problems in least squares, Q. Appl. Math., 2, 164 -168.

Lines, L. R. & Treitel, S., 1984. Tutorial: a review of least-squares inversion and its application to geophysical problems, Geophys. Prospect., 32, 159-186.

Marquardt, D. W., 1970. Generalized inverses, ridge regression, biased linear estimation and nonlinear estimation, Technometrics, 12, 591-612.

Muller, W., 1982. Unified calculation of the magnetotelluric impedance and admittance tensor elements, Geo. Jb., 23, 251-259.

Oldenburg, D. W., Whittall, K. P. & Parker , R. L., 1984. Inversion of ocean bottom magnetotelluric data revisited, J. geophys. Res., 89, 1829-1833.

Parker, R. L., 1983. The magnetotelluric inverse problem , Geophys. Surveys, 6, 5 -25.

Reddy, I. K. & Rankin , D., 1972. On the interpretation of magnetotelluric data in the plains of Alberta, Can. J. Earth Sci., 9, 514-527.

Shankland, T. J. & Ander, M. E., 1983. Electrical conductivity , temperatures, and fluids in the lower crust, J. geophys. Res., 88, 9475-9484.

Sims, W. E., Bostick, F. X. J. & Smith, H. W., 1971. The estimation of magnetotelluric impedance elements from measured data, Geophysics, 36, 938-942.

Vozoff , K., 1972. The magnetotelluric method in the exploration of sedimentary basins, Geophysics, 37, 98-141.

Weidelt, P., Muller, W., Losecke, W. & Knodel, K., 1980. Die Bostick transformation, in Protokoll uber das Kolloquium 'Elektromagnetische Tiefen forschung', pp. 227-230, eds Haak, V. & Homilius, J., Berlin.

Table 1. (a) Results of 1-D inversion procedures, for site 2 (CK). Three-layer models consisting of resistivity (ρ, Ω m) and thickness (t, km). Solution 1 obtained by the method of Fischer & Le Quang (1981). Solution 2, with standard errors (SE) obtained by ridge regression. Chi-square (χ^2) is a measure of misfit between model and data.

(i)

	Solutions		
	Solution 1	Solution 2	SE (Solution 2)
ρ_1	64.08×10^3	188.95×10^3	50.20×10^3
ρ_2	11.03	8.18	11.69
ρ_3	276.65	286.83	166.92
t_1	26.10	28.08	3.32
t_2	5.40	3.95	5.62
χ^2	20.0	20.9	

(ii) Parameter correlation matrix (solution 2)

	ρ_1	ρ_2	ρ_3	t_1	t_2
ρ_1	1.00				
ρ_2	0.30	1.00			
ρ_3	−0.31	−0.58	1.00		
t_1	−0.19	−0.85	0.78	1.00	
t_2	0.26	0.99	−0.50	−0.81	1.00

(b) Results of 1-D inversion procedures, for site 3 (KL). Three-layer model consisting of resistivity (ρ, Ωm) and thickness (t, km). Solution 1 obtained by the method of Fischer & Le Quang (1981). Solution 2, with standard errors (SE) obtained by ridge regression. Chi-square (χ^2) is a measure of misfit between model and data.

(i)

	Solutions		
	Solution 1	Solution 2	SE (solution 2)
ρ_1	5.61×10^3	11.28×10^3	3.20×10^3
ρ_2	7.66	12.34	12.08
ρ_3	238.73	245.60	88.64
t_1	15.70	14.89	2.85
t_2	4.80	7.96	8.29
χ^2	22.4	22.96	

(ii) Parameter correlation matrix

	ρ_1	ρ_2	ρ_3	t_1	t_2
ρ_1	1.00				
ρ_2	0.35	1.00			
ρ_3	−0.13	0.22	1.00		
t_1	−0.36	0.97	−0.04	1.00	
t_2	0.32	0.99	0.28	−0.95	1.00

(c) Results of 1-D inversion procedures, for site 4 (WK), as per (a).

(i) Solutions

	Solution 1	Solution 2	SE (solution 2)
ρ_1	3.19×10^3	1.40×10^3	0.42×10^3
ρ_2	9.70	7.08	2.38
ρ_3	186.67	163.90	21.84
t_1	7.80	8.39	0.71
t_2	7.70	5.32	1.90
χ^2	30.9	22.3	

(ii) Parameter correlation matrix

	ρ_1	ρ_2	ρ_3	t_1	t_2
ρ_1	1.00				
ρ_2	0.01	1.00			
ρ_3	–0.21	–0.06	1.00		
t_1	–0.17	0.92	0.35	1.00	
t_2	–0.02	0.99	0.01	–0.89	1.00

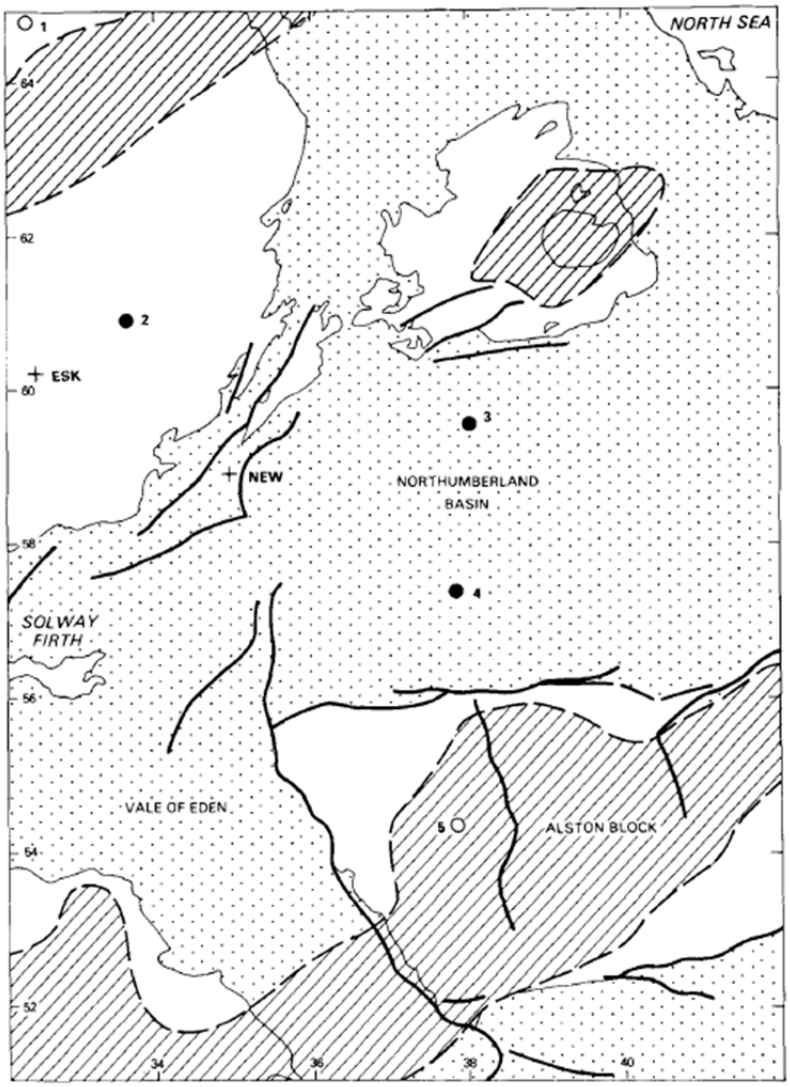

Figure 1. Site locations and geology : site 1 , Early burn (EB); site 2 , Craik (CK); site 3, Keilder (K L) ; s i t e 4, Wark (WK); site 5, Pennine Way (PW). Solid dots refer to the central three sites (2, 3 and 4). ESK (Eskdalemuir) and NEW (Newcastleton) are other sites referred to in the text. Shading indicates a region underderlain by granite batholiths. Stippled areas arc underlain by substantial thicknesses of post-Caledonian sedimentary rock . Coordinate values are National Grid; multiply by 10 for kilometre scale.

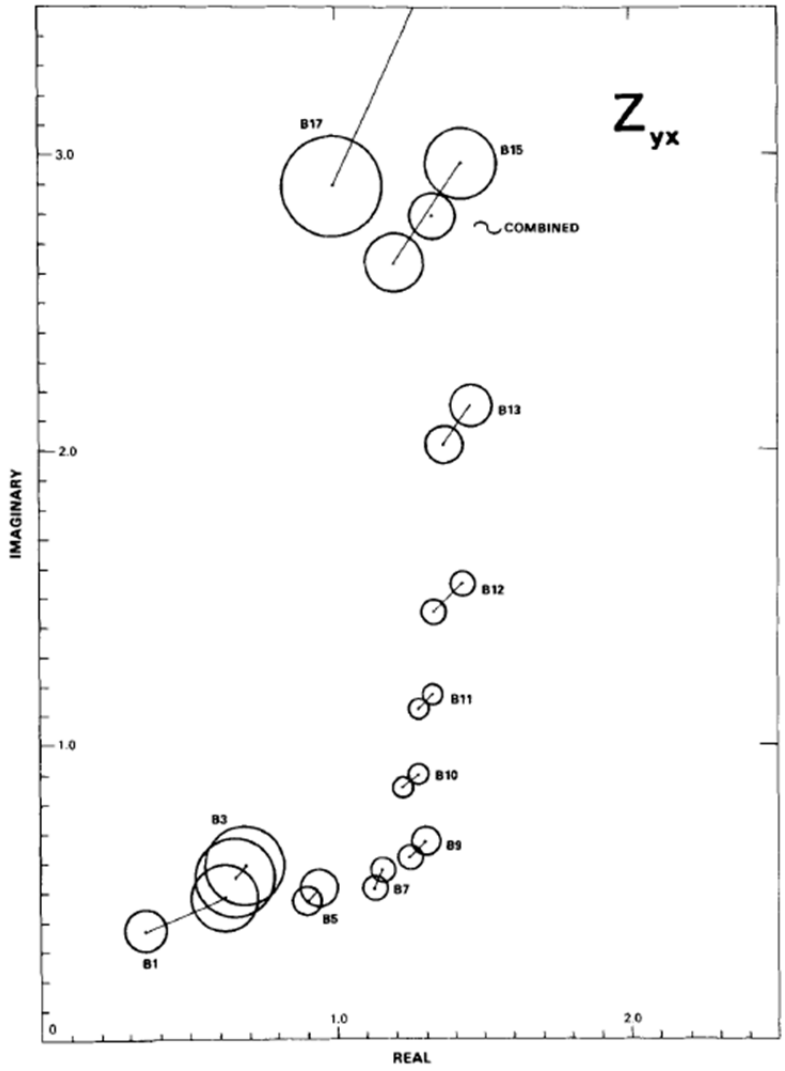

Figure 2. Plot of upward- and downward-biased estimates of the impedance element Zyx, in the complex plane for site 3 (KL). The results for 11 period bands (B1 –B17) are shown from a total of 18. Period bands range from 7200 s (B1) to 30 s (B17). The random errors associated with each estimate are used to define the circles of confidence (68 per cent confidence limits) of the weighted mean estimates.

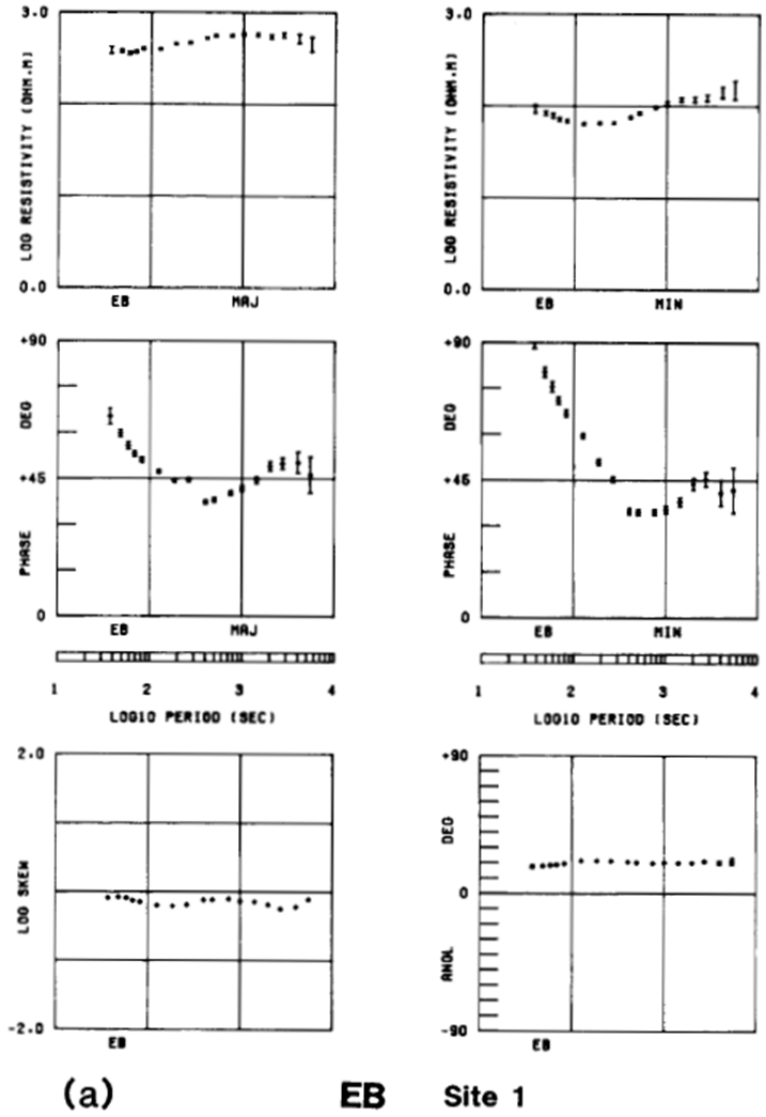

Figure 3 Magnetotelluric results in a log period (1--4) scale. For each site, the plots display log (apparent resistivity) and phase in the major (MAJ) and minor (MIN) principal directions, together with the azimuth of the major axis of the rotation ellipse (ANGL, measured in degrees clockwise from magnetic north) and the logarithm of the skewness coefficient. (a) Site 1-EB, (b) site 5-PW, (c) site 2-CK, (d) site 3-KL, (e) site 4-WK.

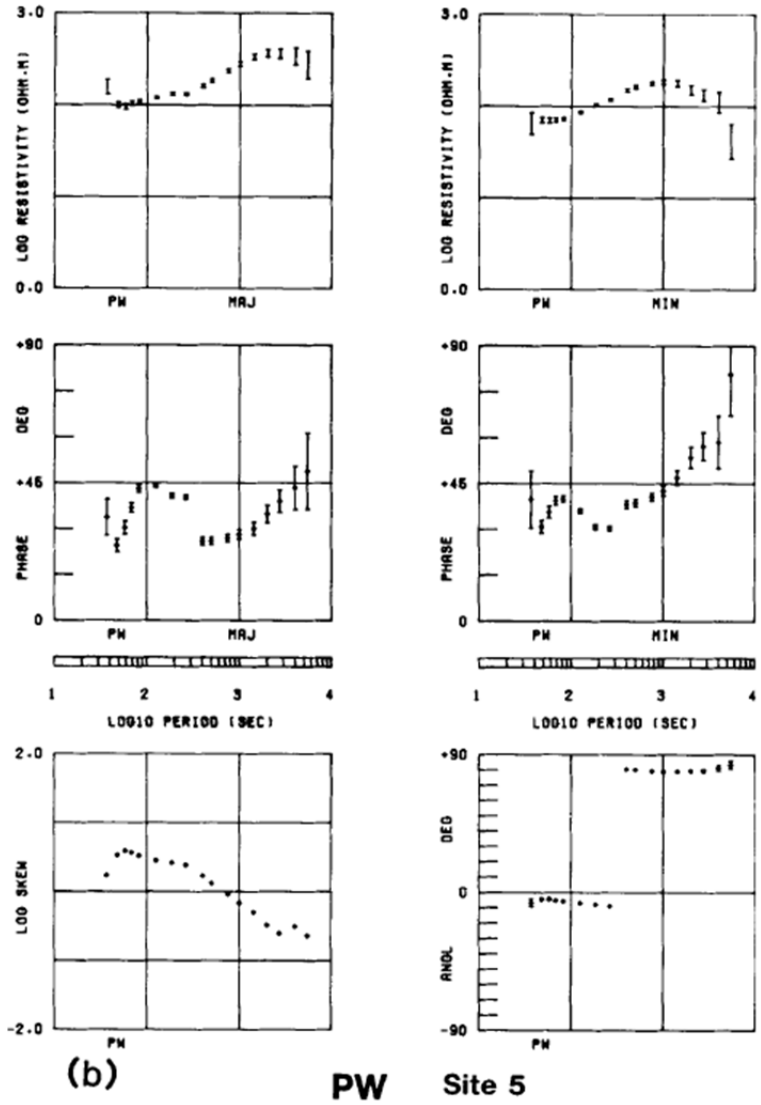

Figure 3b. As previous

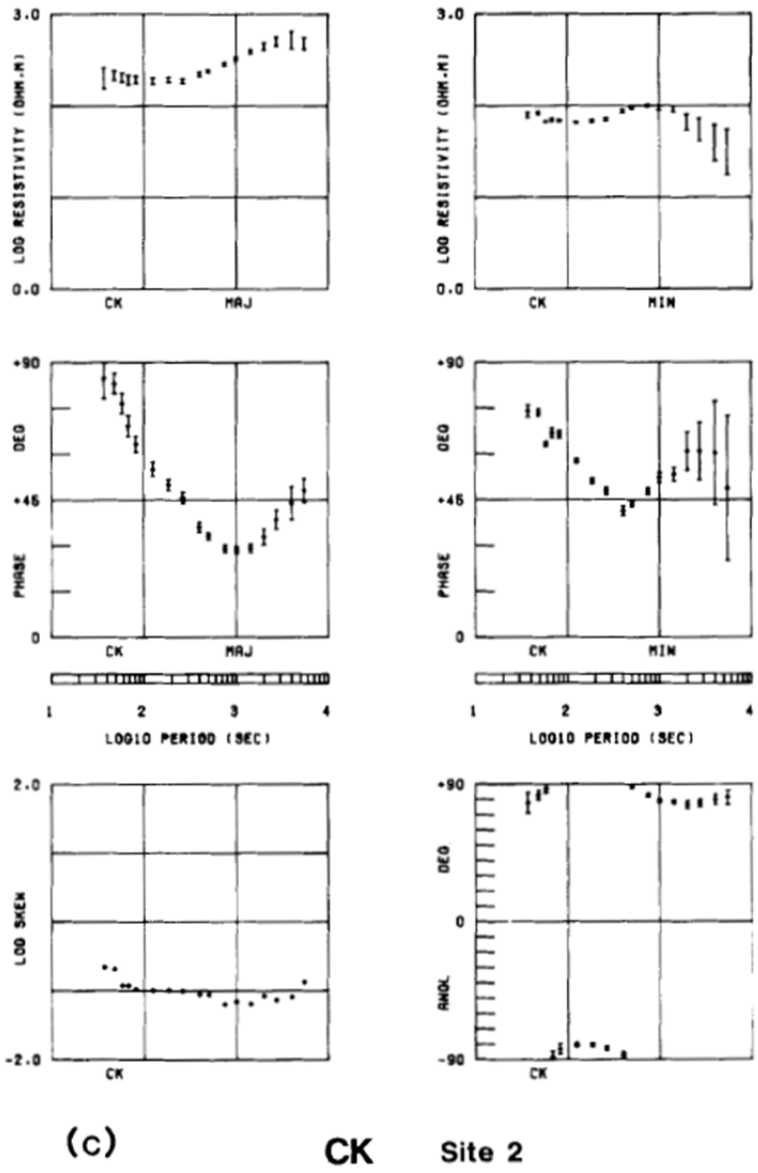

Figure 3c. As previous.

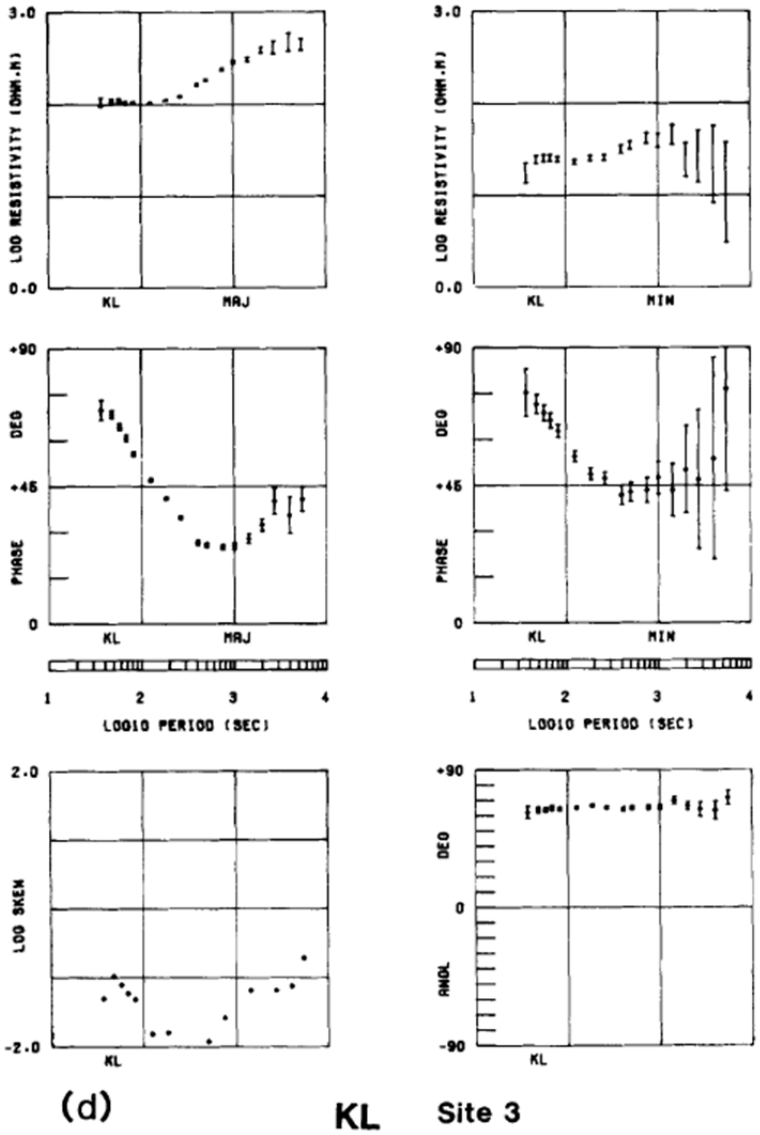

Figure 3d. As previous.

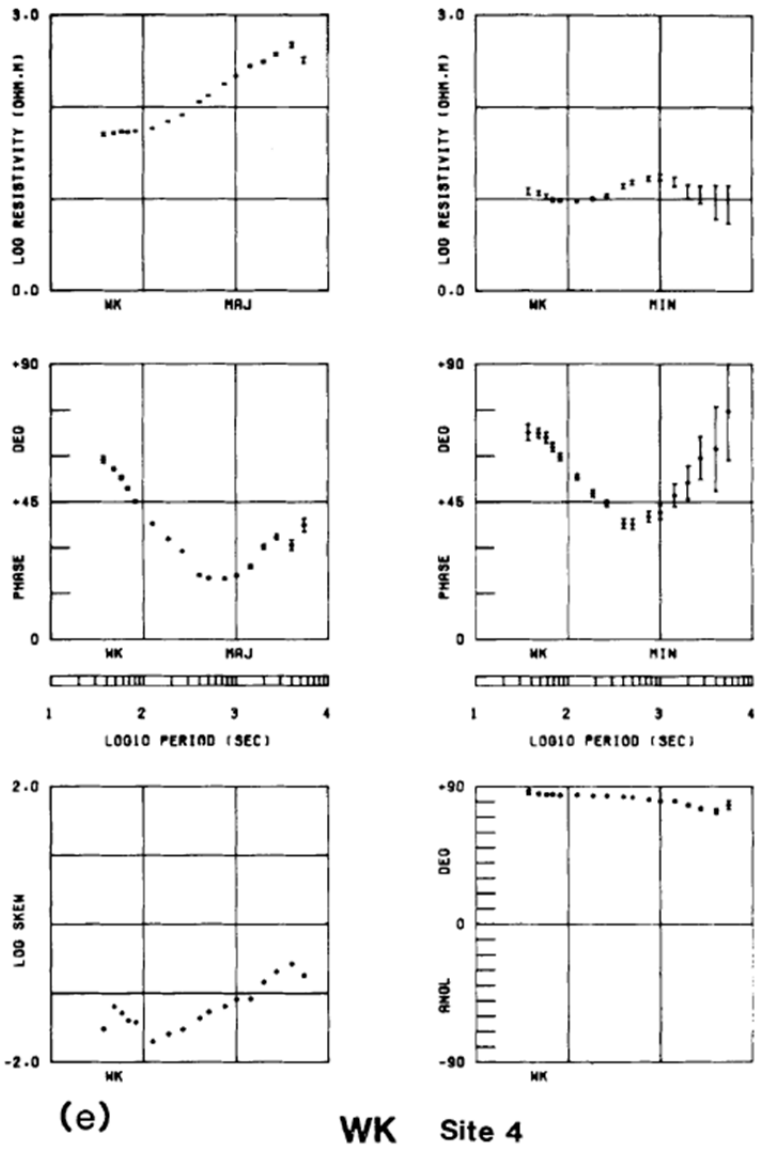

Figure 3e. As previous.

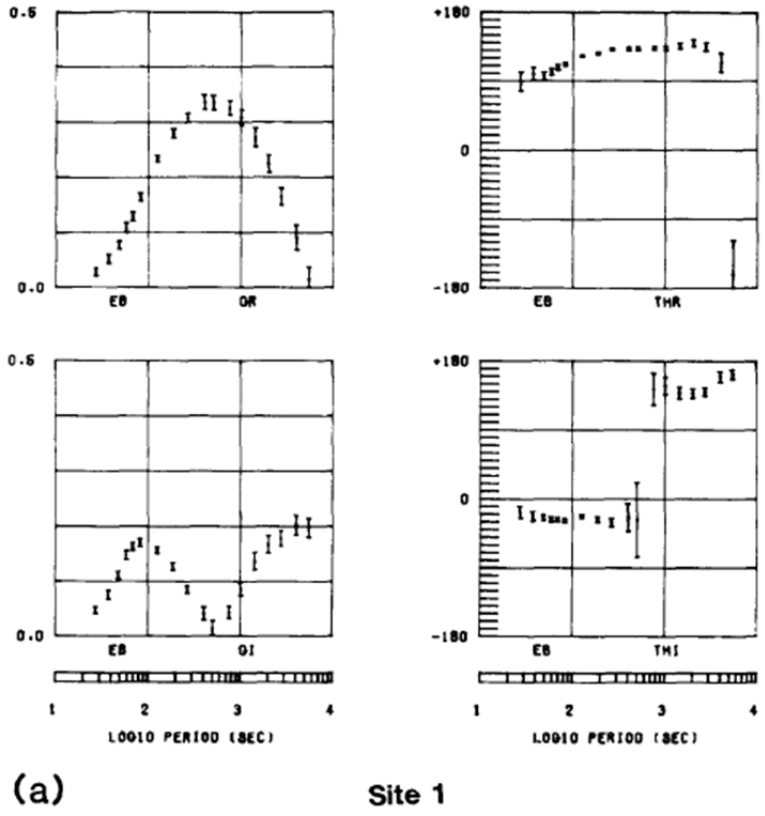

Figure 4. Induction arrow results across the region on an equivalent period scale to that of Fig. 3. Upper two plots show the real induction arrow (amplitude, azimuth) and the lower two plots show the imaginary induction arrow (amplitude, azimuth) for each case. (a) Results at site 1. (b) Results at sites 2, 3, 4 and six other sites in the vicinity of the Northumberland Basin, overlaid. (c) Results of site 5 and nine other sites on the Alston Block, overlaid.

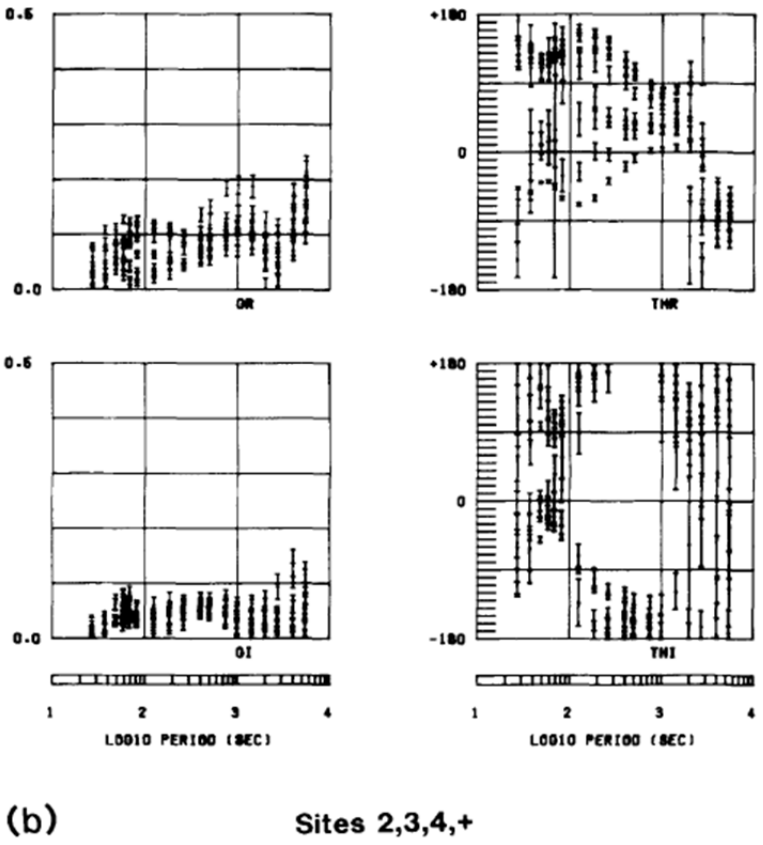

(b) Sites 2,3,4,+

Figure 4b. As previous.

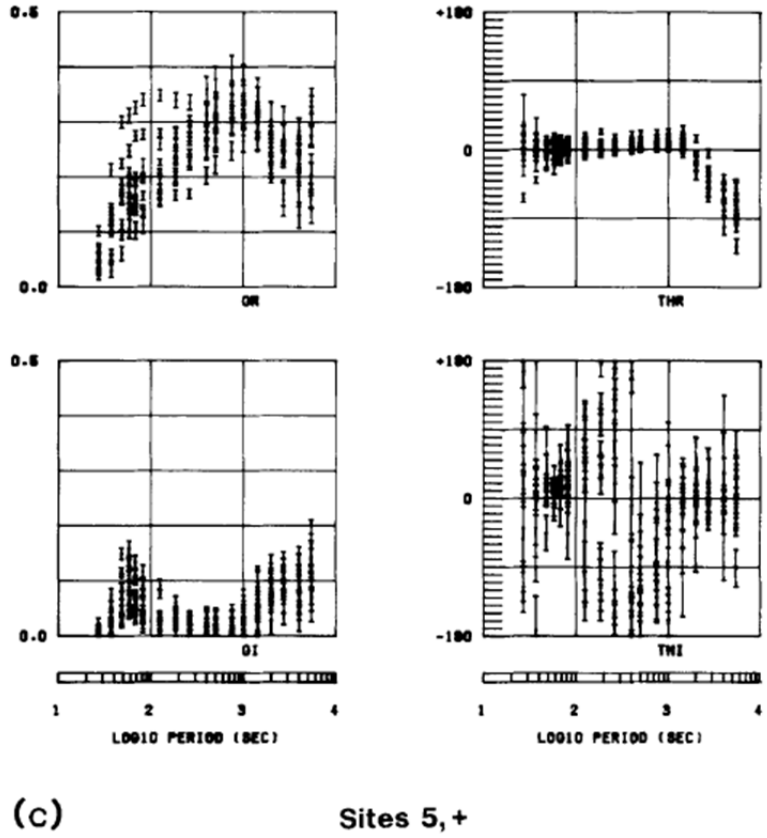

(c) Sites 5, +

Figure 4c. As previous.

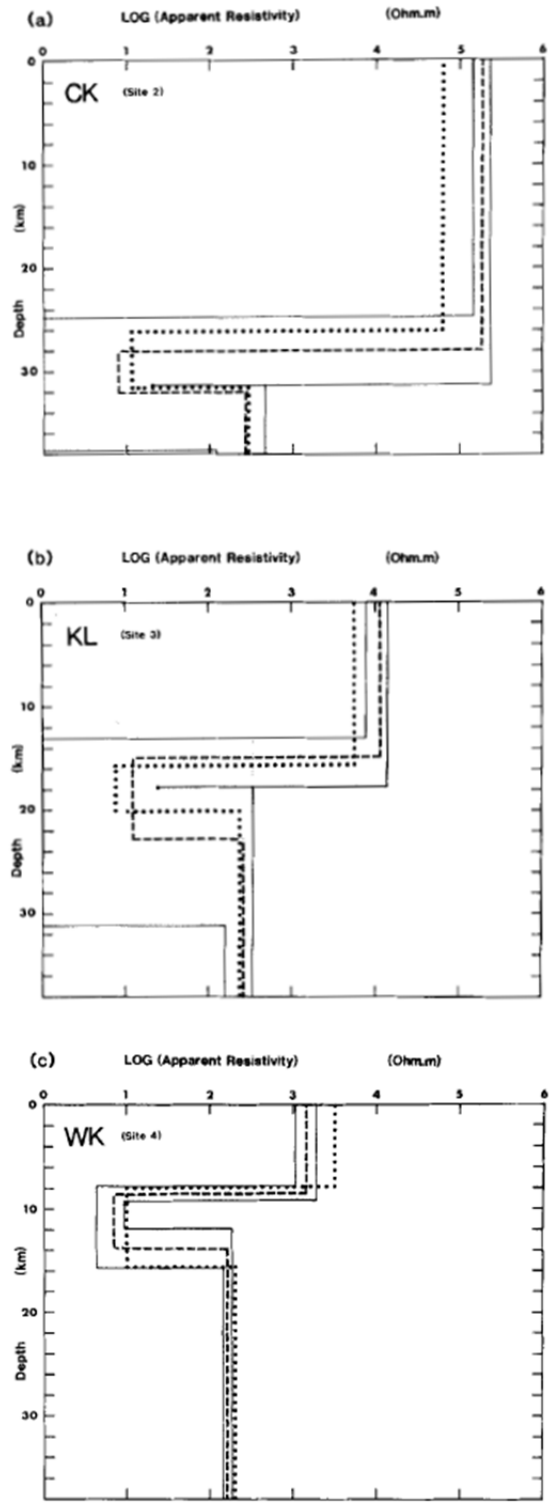

Figure 5. Three-layer crustal models of variation in apparent resistivity with depth produced by two inversion schemes. Dotted line refers to optimum model produced by solution 1, referred to in the text. Dashed line refers to the optimum model produced by solution 2. The shaded region defines the standard errors associated with each parameter obtained from solution 2. (a) Site 2 (CK), (b) site 3 (KL), (c) site 4 (WK).

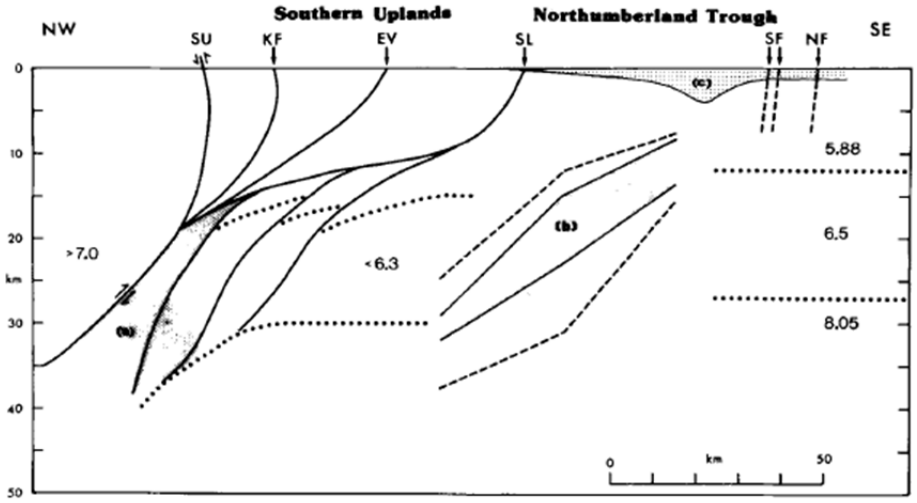

Figure 6. Three models of deep crustal structure beneath southern Scotland and northern England resolved along a synthetic NW-SW profile. Underlying the Southern Uplands is a simplified tectonic model proposed by Leggett et al . (1981). Numbers refer to seismic P-wave velocities in km.s^{-1}. The lower crust of velocity < 6.3 is referred to as under thrusting English basement while zone (a) is referred to as metamorphosed relics of ocean crust. Zone (b) is the depth profile of the highly conducting layer provided by the present study. The dotted line refers to conservative error bounds on the depth to, and thickness of, the layer. The crustal velocity structure in the SE under northern England is taken from Bott et al . (1984). Region (c) is the Carboniferous Northumberland Basin. Vertical exaggeration is X 2. SU , Southern Uplands Fault; KF , Kingledores Fault; EV, Ettrick Valley Fault; SL, Solway Line; SF, Stublick Faults; NF, Ninety Fathom Fault. All later Caledonian granites are ignored.